SEISMIC ANALYSIS OF MASONRY BUILDINGS USING EXPLICIT INTEGRATION METHOD

Elesban Nochebuena-Mora

PhD Student
ISISE, University of Minho
Portugal
enochemora@gmail.com

Nuno Mendes

Post-Doc Researcher
ISISE, University of Minho
Portugal
nunomendes@civil.minho.pt

Paulo B. Lourenço

Full Professor
ISISE, University of Minho
Portugal
pbl@civil.minho.pt

ABSTRACT

The Finite Element Method (FEM) has become one of the most used numerical tools for advanced modelling of unreinforced masonry buildings. Implicit methods are often used to solve the set of equations in structural problems. Although they are reliable given their precision, the computational effort is high and strongly dependent on the convergence criteria. These difficulties increase when structural problems involve nonlinear dynamic responses, such as the seismic analysis of masonry buildings, where the quasi-brittle behaviour of the material hinders the convergence of the solution. Explicit methods can overcome this obstacle, as they were developed for mechanical problems with severe geometric and material discontinuities. The explicit solvers require a significantly small time increment to produce accurate results, leading to analyses with many thousands of steps, but with less computational effort. However, some parameters affect the stability of the solution and the accuracy of the results. This article addresses these parameters and their influence on the dynamic response of an unreinforced masonry building. Four FEM models were created using Abaqus/Explicit to perform a sensitivity analysis. The number and type of elements were varied (linear fully integrated elements and reduced integration elements with hourglass control), aiming at evaluating their effect on the energy balance, which is a parameter that controls the quality of the solution.

Keywords: Hourglass, energy balance, artificial energy, unreinforced masonry.

1. INTRODUCTION

The Finite Element Method (FEM) is a common computational tool used in civil engineering research. In the implicit solvers, a solution to the set of equations involves iteration until a convergence criterion is satisfied for each increment. When the problem includes strong nonlinearities, many iterations are usually needed to solve for an increment, or even, there is no convergence. These issues are overcome by the explicit solvers since they do not use an iterative process to solve the system of equations. Nevertheless, they need a large number of small time increments to obtain accurate results [1]. The explicit method has a great capacity and advantage in analysing transient dynamics of a high nonlinear system including large deformation, large rotation, nonlinear material, contact, and crash [2].

It is a wide practice the use of FEM models with implicit solvers in the assessment of historical unreinforced masonry buildings. Although the power and accuracy of the tool have been already demonstrated, the computational cost to run nonlinear dynamic analyses is still an inconvenience, mainly for large models, in which local failures of the material cause convergence difficulties.

Explicit solutions for modelling unreinforced masonry walls and buildings have barely been used. For example, Tarque et al. [3] simulated the experimental campaign of an adobe building tested on a shake table obtaining acceptable results. Yang [4] performed an extensive study comparing explicit and implicit methods for solving dynamic problems involving quasi-brittle materials, demonstrating that both procedures have similar results if the time increment in the explicit solver is small enough. Noor-E-Khuda et al. [5] reproduced the out-of-plane behaviour of unreinforced masonry walls with different configurations and boundary conditions tests in the laboratory.

In the present work, Abaqus/Explicit [6] is used to perform a parametric analysis of a partial model of an unreinforced masonry building. The scope is to assess the response dependency on the type of element and the refinement of the mesh during a seismic analysis with strong accelerations. Given that the explicit method deals with dynamic problems, the conservation of energy is a key aspect to consider for the reliability of the results. Therefore, the evaluation takes into account the energy balance. First, in the dead load application kinetic energy is an important factor, and second, during the seismic analysis, the balance between external work, total energy, internal energy and artificial energy plays an important role.

2. EXPLICIT METHOD FOR FEM MODELS

In general, the explicit integration method uses the central difference operator to integrate the equation of motion, solving the problem without formation and inversion of the stiffness matrix, unlike the implicit solvers. Therefore, each time increment is computationally inexpensive to solve [2,5]. The explicit dynamic method is conditionally stable, meaning that, to produce accurate results, the time increment Δt must be smaller than the limiting time increment, which is related to the highest frequency of the system ω_{max}, material property and length of the element [2]. Since the time is quite small, the analysis requires thousands

of increments, which is inexpensive as the equations are not solved simultaneously. The stability limit is calculated using Equation (6) (see Section 5). Since it is not feasible to calculate the exact value of ω_{max}, conservative estimates are applied instead, assuming the concept of a dilatation wave travelling along the element length L^e:

$$\Delta t = L^e \sqrt{\frac{\rho}{E}} \tag{1}$$

where E is the Young's modulus and ρ is the material density [7]. Abaqus/Explicit automatically calculates the increment time and reduces it by a factor between $1/\sqrt{3}$ to 1 for a three-dimensional model [8].

3. DESCRIPTION OF THE BUILDING PROTOTYPE

Figure 1 presents the layout of the building selected for the analysis. It is a prototype of the typical viceregal dwellings built in the 17th and 18th centuries in many cities in Mexico during the Spanish colony. The prototype consists of two floors with interstory height that varies from 4.95 to 5.10 m. The rooms surround two patios, and doors and windows are aligned. The thickness of the walls varies from 0.90 m (façade) to 0.60 m (inner walls). The use of diverse types of volcanic stones extracted from quarries was a widespread practice in the center of the country. Rubble masonry was used in the construction of foundations and walls, while dressed stones were used for columns and arches. Both floors and roof are flat slabs composed of a large set of timber joists (0.15 x 0.20 m), disposed perpendicular to the façade and with a spacing of 0.30 m, that support a layer of brick, compacted earth, and pavement. There is no mechanical connection between the joists and walls, relying only on frictional resistance to avoid the sliding of joists.

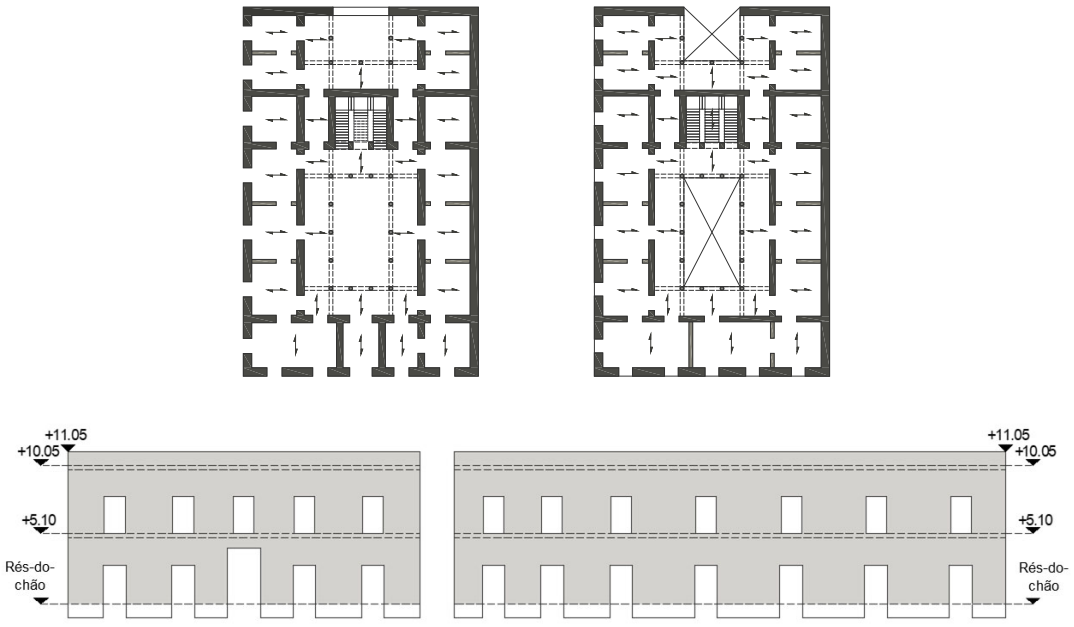

Figure 1. Building prototype of the viceregal dwellings in Mexico.

4. MECHANICAL PROPERTIES

Density, Young's modulus and compression strength applied for masonry were obtained from Chávez et al. [9], who performed tests on some samples taken from churches in the centre of Mexico. Regarding the tension properties, the strength was assumed 10% of the compression strength. Foundation and walls have the same properties since both were normally built with rubble masonry and similar material quality. Timber for joists and lintels is assumed to remain in the linear range during all the analysis since no damage in these elements is expected. Density and Young's modulus for timber were taken from Guzmán [10]. Table 1 presents the mechanical properties of masonry and timber.

Table 1. Mechanical properties

	Density [kg/m^3]	Young's modulus [N/m^2]	Poisson's ratio	Compression strength [N/m^2]	Tension strength [N/m^2]	Tension fracture energy [N/m]
Rubble masonry	1794	1.43e+09	0.2	1.90e+06	1.90e+05	50
Timber	610	8.8e+09	0.3			

4.1 Constitutive law for masonry

The material model adopted for the analyses was the concrete damage plasticity (CDP) model since it can describe the nonlinear behaviour of other quasi-brittle materials, including masonry, as demonstrated by D'Altri et al. [11]. This model is provided in Abaqus and has been implemented to simulate the response of several unreinforced masonry buildings for nonlinear static and dynamic analyses [3,12,13].

This model allows the analysis of materials with different strength in tension and in compression, assuming two damage parameters to describe the tensile cracking ($0 \leq d_t < 1$) and compressive crushing ($0 \leq d_c < 1$) [14]. The stress-strain relations in uniaxial tension σ_t, and compression σ_c are:

$$\sigma_t = (1 - d_t)E_0\left(\varepsilon_t - \varepsilon_t^p\right),\ \sigma_c = (1 - d_c)E_0\left(\varepsilon_c - \varepsilon_c^p\right) \quad (2)$$

where E_0 is the initial Young's modulus of the material, ε_t and ε_c are the uniaxial tensile and compressive strains, and ε_t^p and ε_c^p are the uniaxial tensile and compressive plastic strains (Figure 2). Based on the values in Table 1 the stress-strain compression and tension curves were calculated (Figure 3). The damage parameters were obtained with an approximation given by $d = 1 - \sigma/\sigma_{max}$.

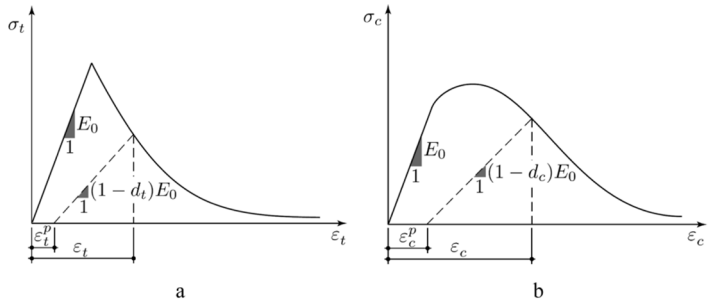

Figure 2. a) Tensile and b) compression uniaxial nonlinear curves (D'Altri et al., 2019).

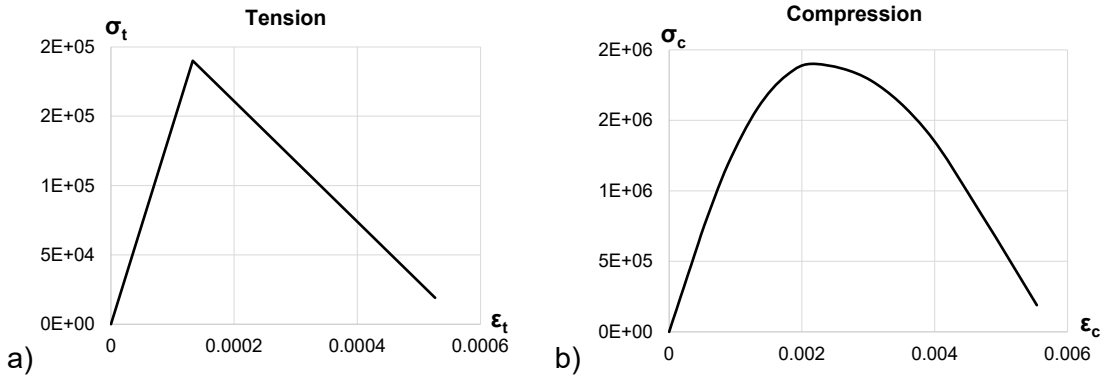

Figure 3. Tensile and compression uniaxial nonlinear curves adopted in the analysis.

CDP model requires other five parameters to describe the yield surface. These parameters are the dilatancy angle ψ, for which a value of 10° was adopted. The ratio between the biaxial and uniaxial compressive strength f_{b0}/f_{c0}, assumed equal to 1.16. The parameter K, set to 2/3, as recommended by Abaqus [8]. The viscoplastic regularization (viscoplastic parameter), which is used (with a value larger than zero) to avoid convergence problems in implicit analysis, was assumed as zero since the explicit method is applied in this case. The last parameter is the eccentricity, considered as 0.1. For further details, the reader is referred to [8,14].

5. RAYLEIGH DAMPING IN THE EXPLICIT METHOD

Abaqus only allows Rayleigh damping for explicit solutions [8]. This damping type assumes that the damping matrix $\boldsymbol{C}$ is a combination of the mass $\boldsymbol{M}$ and stiffness $\boldsymbol{K}$ matrices with the respective damping parameters [15]:

$$\boldsymbol{C} = \alpha \boldsymbol{M} + \beta \boldsymbol{K} \tag{3}$$

For each angular frequency of the system ω_a, the effective damping ratio is related to the mass damping parameter α and the stiffness damping parameter β through:

$$\xi = \frac{\alpha}{2\omega_a} + \frac{\beta \omega_a}{2} \tag{4}$$

The mass damping parameter controls the low frequencies while the stiffness damping parameter dominates the high frequencies. To calculate α and β, the fundamental frequency of the structure ω_0 and a higher frequency ω_{max} that contributes considerably to the

response are selected. If the modes associated with those frequencies have the same damping ratio, which is reasonable based on experimental data, then:

$$\alpha = \xi \frac{2\omega_0\omega_{max}}{\omega_0+\omega_{max}};\ \beta = \xi \frac{2}{\omega_0+\omega_{max}} \quad (5)$$

In order to guarantee numerical stability in the explicit method, small steps are required for the accurate integration of the highest eigenfrequency ω_{max}. Such steps should be smaller than the stability time increment given by:

$$\Delta t \leq \frac{2}{\omega_{max}}\left(\sqrt{1+\xi_{max}^2}-\xi_{max}\right) \quad (6)$$

if ω_{max} is high, $\frac{\alpha}{2\omega_{max}} \to 0$, thus α does not affect the time increment significantly. However, the term related to β can reduce the time increment and even can make the analysis unattainable for large models. To avoid this problem and minimize the computational cost, stiffness proportional damping is usually taken as zero [16] and only the mass proportional damping is applied [17].

Thus, in this study only the α parameter was calculated while the β parameter was set to zero in all the analyses. Regarding the damping ratio, it is normally considered as 3% for unreinforced masonry buildings.

6. NUMERICAL MODEL

Since the building prototype is too large, a partial and simplified model was adopted for the nonlinear dynamic analysis (Figure 4). Foundation, walls and lintels were modelled with solid elements. The joists (beam element type B21) were also included in the model to evaluate the effects of the floor and roof on the response of the building. During a cyclic load, for example in an earthquake, the joists may slide out of the walls when tensional forces develop and cannot penetrate if there is compression. Thus, translator connections with nonlinear behaviour (low stiffness for tension and high stiffness for compression) simulate the link between walls and joists.

Based on the eigenvalues analyses, previously performed, it was possible to determine that the dynamic properties of the partial and complete model remain the same for the out-of-plane behaviour of the façade.

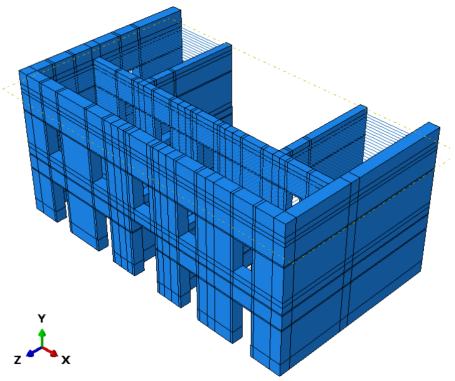

Figure 4. Geometry of the partial model.

6.1 Mesh and element type

The explicit solution in Abaqus only includes linear solid elements with reduced integration and hexahedral elements fully integrated [8]. Fully integrated elements use two integration points in each direction. Despite the high accuracy of this type of element, shear locking affects their performance when subjected to bending loads, since they are numerically stiffer than they actually should be [18]. Increasing the number of elements does not avoid the shear locking. Therefore, they are recommended when the actions will produce minimal bending. Reduced integration linear elements have a single integration point located at the centroid. The advantage of using only one integration point per element is that the computational time is reduced [19], and shear locking is not presented. However, they have a spurious behaviour called hourglassing that can propagate in coarse meshes producing meaningless results. When the element is subjected to certain deformations, the neutral axes remain unchanged in length and rotation, so the location of the integration point is not altered and therefore any variation in the stress-strain field is calculated (Figure 5). As a result, the element is free to distort because no strain energy is produced to counteract such deformation [18]. Hourglass effect is prevented by using at least four elements through the thickness [19] when structures carry bending loads. Additionally, an artificial stiffness (represented as artificial energy) introduced by the software avoids large deformations.

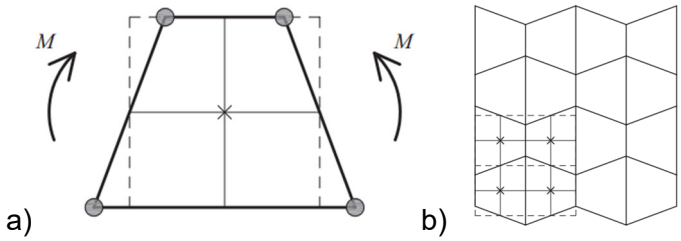

Figure 5. a) Hourglass mode and b) propagation of the hourglass effect [18].

Four models with different meshes were generated to evaluate the effects of the type and size of the elements on the results. Model 3F has three fully integrated elements (C3D8) through the thickness of the façade, whereas Model 3R, Model 4R and Model 6R contain three, four and six reduced integration elements (C3D8R), respectively, along the thickness of the elements where bending may occur, as shown in Figure 6.

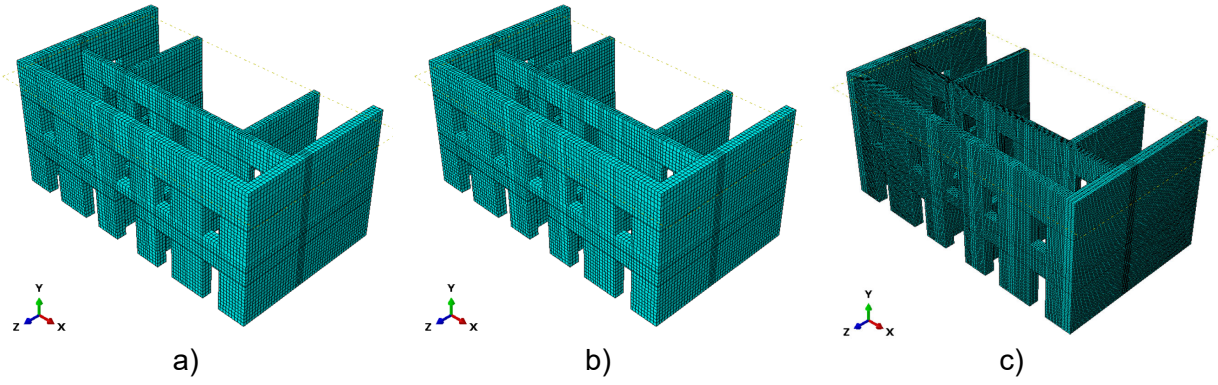

Figure 6. a) Model 3F and Model 3R (41 660 elements), b) Model 4R (98 043 elements), and c) Model 6R (210 250 elements).

7. ENERGY BALANCE

Energy balance is an important parameter in explicit solutions that can help, by means of comparisons between various energy components, to assess the quality of the model and the reliability of the results. For the presented case, the energy conservation equation is:

$$E_I + E_V + E_K - E_W = E_{total} = 0 \quad (7)$$

where E_I is the internal energy, E_V is the energy dissipated by damping mechanism (including the material damping), E_K is the kinetic energy, and E_W is the work done by external loads. Internal energy is the sum of recoverable elastic strain energy, the energy dissipated through plasticity, the energy dissipated through viscoelasticity or creep of the materials, the energy dissipated through damage, and artificial strain energy. In numerical methods, E_{total} is only an approximation to a constant equal to zero, generally with an error of less than 1% [8], i.e., the ratio $E_{total}/E_W < 1\%$ during the complete analysis.

7.1 Artificial energy and hourglass controls

If reduced integration elements are used, the FEM solver adds artificial forces to control the hourglass effect in parts of the model that start to deform. Artificial stiffness is converted into artificial energy, which can increase during the analysis to amounts comparable to physical energies [20]. This is one of the main sources of errors in the results. A common criterion is that the artificial energy should be small relative to the internal energy, no more than 1% [7]. However, this rule is more appropriate for quasi-static analysis, where there are small deformations, and the velocity of load application is relatively slow. For dynamic problems, a range between 5 to 10% is assumed as a reasonable limit for engineering applications [2,21,22].

Numerical solvers usually adopt viscous damping or small elastic stiffness added to the stiffness matrix to stop the formation of anomalous modes [2]. In this regard, Abaqus/Explicit has various numerical techniques to suppress hourglass appearing and propagation [8]. Based on previous analyses carried out on the FEM models and the sensitivity analysis performed by [19], two hourglass controls were applied to the three models with reduced integration elements. The enhanced approach minimizes the hourglass modes of the elements connected to the floor and roof, while stiffness (displacement hourglass set to 0.01) constraints the rest of the elements. The combination reduces significantly the artificial energy and supresses spurious distortions of the solid elements for the present case study.

8. DYNAMIC ACTIONS

First, the models were subjected to self-weight. An explicit solution is always a dynamic solution. Thus, the application of the dead load must be carried out with a quasi-static analysis with a low velocity. The gravity was applied with a smooth function with a time of 1 s, which allows the dilatation wave to travel along the complete model. The results are feasible if the kinetic energy of the system is equal or close to zero during the time application.

Several nonlinear dynamic analyses were performed to compare the behaviour of the four models under different intensities of ground acceleration (10, 25, 50 and 75%). The explicit solver is more efficient when the dynamic actions are introduced as velocities instead of accelerations or displacements [8]. Figure 7 shows the North-South component of the Emilia Romagna's earthquake recorded in the seismic station in Mirandola (Italy), on May 29th, 2012 [23]. The velocity was applied only in one direction to produce the out-of-plane collapse of the façade.

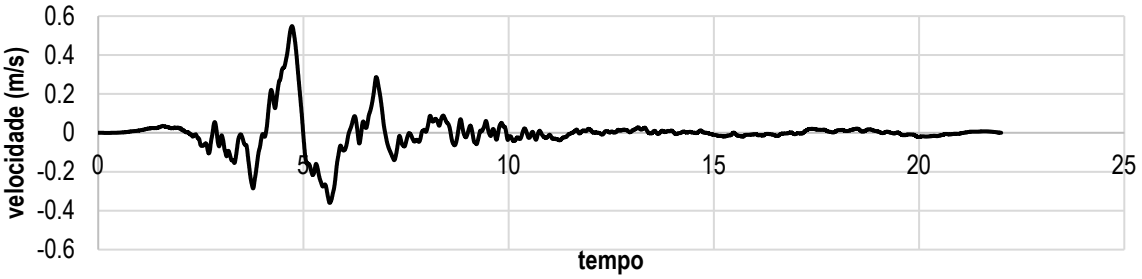

Figure 7. Seismic signal used in the analyses.

9. RESULTS

The performance of the models was evaluated in terms of energy, running time, displacement of a control point (located at the top-centre of the façade), and a qualitative assessment of the damage. The ratio between the total energy and external work must be less than 1% and the ratio between the artificial energy and the internal energy should remain below 5%. Table 2 presents a summary of the main results regarding running time and energy balance.

Table 2. Summary of the main results.

Intensity	Model 3F		Model 6R			Model 4R			Model 3R		
	Time	TE (%)	Time	TE (%)	AE (%)	Time	TE (%)	AE (%)	Time	TE (%)	AE (%)
10%	22h 57min	0.09	23h 53min	0.26	0.29	8h 45min	0.15	0.15	4h 50min	0.09	0.14
25%	19h 43min	0.23	19h 12min	0.63	1.44	9h 45min	0.36	0.69	4h 49min	0.23	0.56
50%	17h 45min	0.13	23h 27min	0.28	1.99	10h 5min	0.18	2.37	5h 2min	2.77	0.15
75%	2h 45min	0.60	3h 52min	0.15	>5	1h 58min	0.10	>5	59min	0.10	>5

9.1 Seismic record scaled to 10%

In the first set of analyses, the four models remained within the linear range since the intensity of the action was small. Thus, the ratios of energy remain quite below the limits (less than 0.3% for both artificial and total energies as shown in Table 2). The displacement

history of the control point is the same in all the models. However, the running time increases considerably for Model 3F and Model 6R, as expected given the number of elements and integration points.

9.2 Seismic record scaled to 25%

In the first analysis, the damage pattern in all the models is the same. Some parts of the building start developing cracks, mainly in the connection between the façade and orthogonal walls. Given that distortion of elements is larger, the algorithm for hourglass control introduces forces which are reflected in the energy balance. However, both energies are still within the range in all the models (no more than 1.5% for artificial energy and 0.63% for total energy) (Table 2). In terms of displacements, the responses depicted in Figure 8 are almost equal, with some variations for Model 3F at the last half of the seismic excitation. The time for Model 3F and Model 6R is over 19 hours of computation, whereas Model 3R and Model 4R are less than 10 hours.

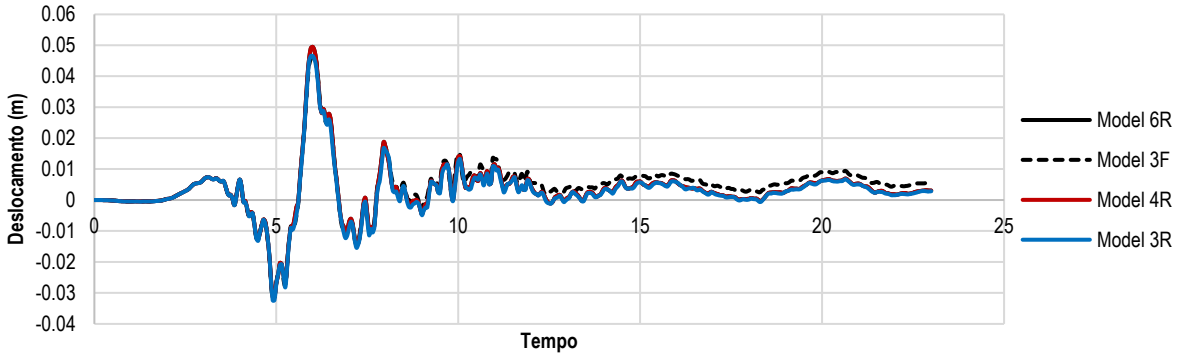

Figure 8. Displacements of the control point for 25% of the seismic action.

9.3 Seismic record scaled to 50%

For the 50% earthquake, the façade completely detached from all the orthogonal walls and the base cracks in the four models (Figure 9). Since the damaged elements had larger deformations, more artificial energy was required to suppress hourglass modes. Model 6R maintained the ratio below 2% while in Model 3R and Model 4R the artificial energy represented more than 2% of the internal energy. Regarding the total energy, it remained below 0.30% in the four models. In terms of time of analysis, Model 6R lasted more than 23 hours to finish the analysis, while Model 4R and Model 3R terminated in less than 10 hours (Table 2). The displacement time history of the control point is similar in all the analyses, with small variations after 10 s (Figure 10).

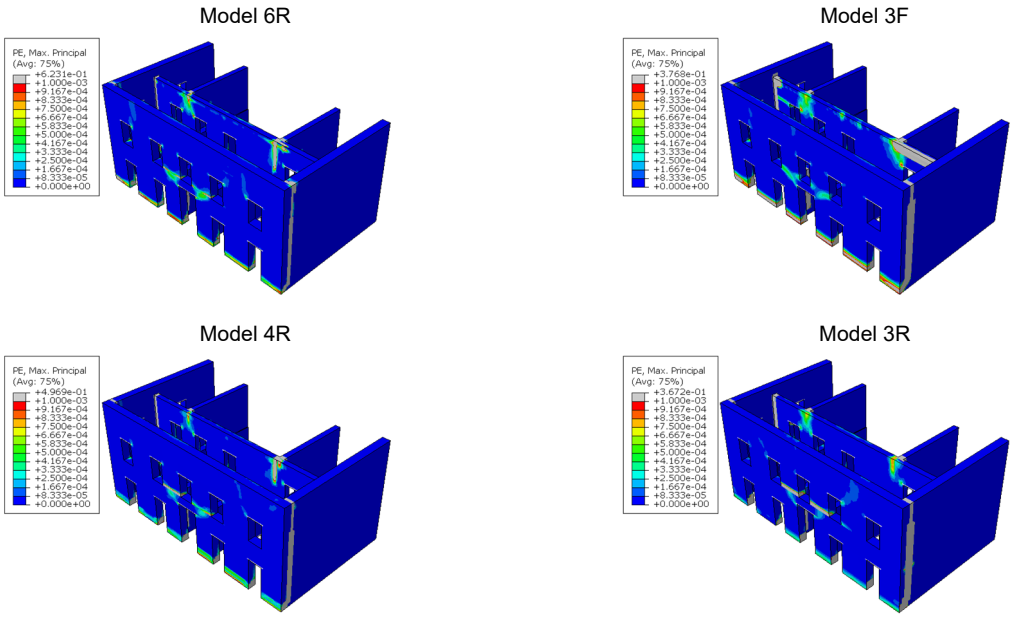

Figure 9. Damage pattern for 50% of the seismic action.

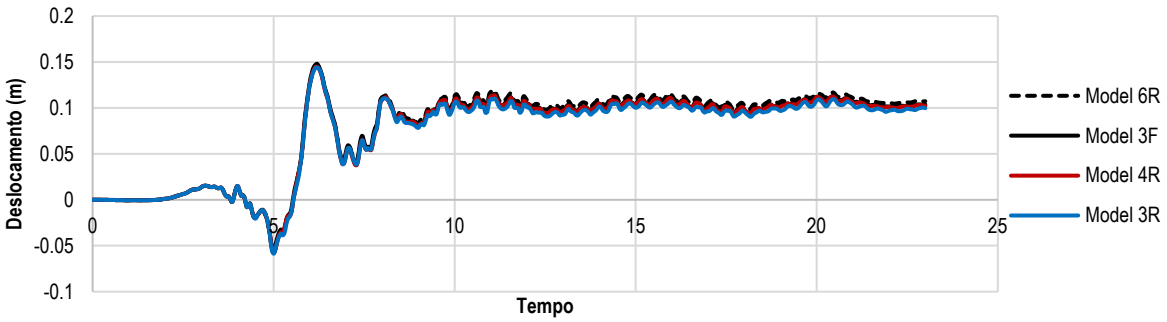

Figure 10. Displacements of the control point for 50% of the seismic action.

9.4 Seismic record scaled to 75%

In the analysis with the 75% of the earthquake, all the models presented similar damage at the façade with cracks developed in the same zones, with exception of Model 3F, which also failed on the roof level (Figure 11). The artificial energy raised over the 5% limit in the three models with reduced integration elements around second 6.2, just right after the largest ground displacement of the signal (Figure 12). Total energy was stable in the three models, however, in Model 3F, there was an abrupted change around second 6.2, which indicates a problem in the solution. The displacements of the control point in the four analyses were similar until second 6.2, when the energies of the system are no longer in balance (Figure 13). At this time, it was assumed that the façade collapsed since the levels of artificial energy indicated high distortion of the damaged elements. To achieve this point of the analysis, Model 6R lasted almost 4 hours, while Model 3R ran less than 1 hour. The other two models were within this range of time.

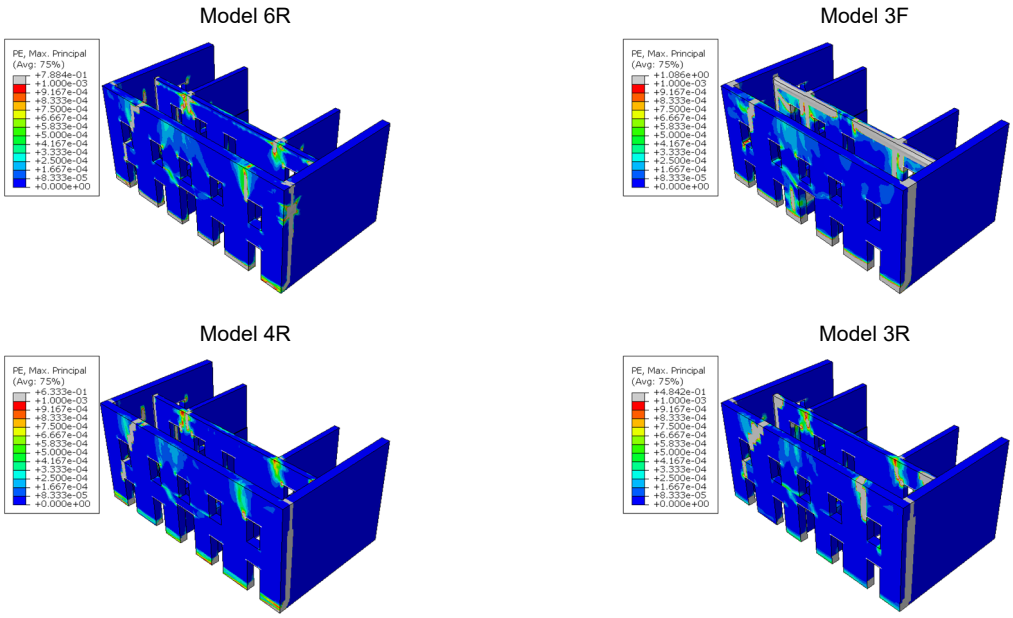

Figure 11. Damage pattern for 75% of the seismic action.

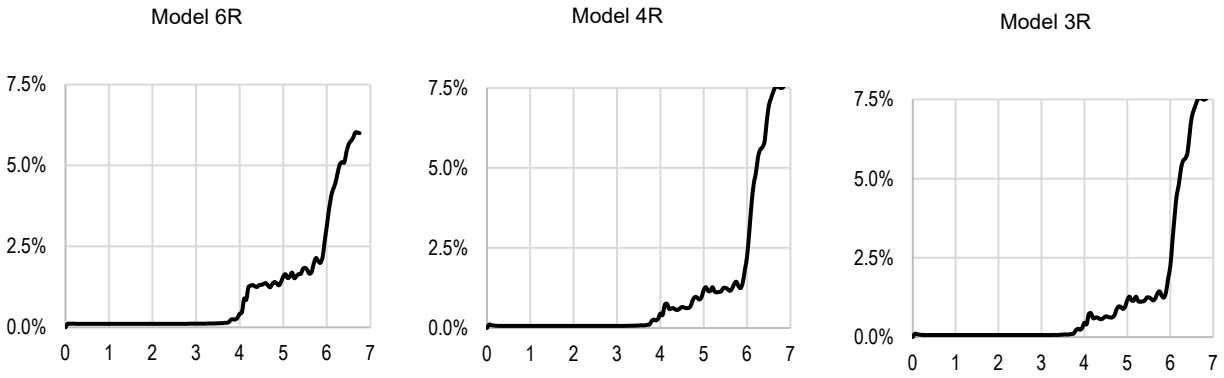

Figure 12. Artificial energy ratio for 75% of the seismic action.

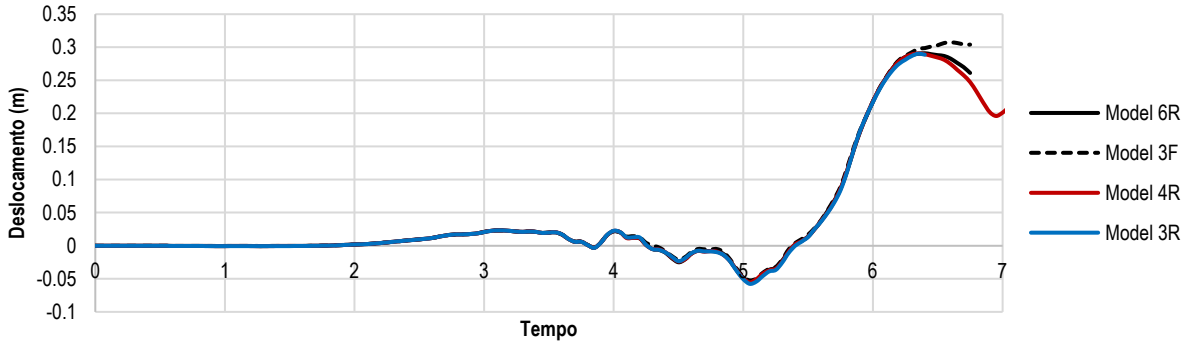

Figure 13. Displacements of the control point for 75% of the seismic action.

Comparing the energy balance, it is clear that, for relatively small distortions, models with a refined mesh (Model 6R) introduce more artificial energy. However, when the nonlinearities increase during the analysis (larger intensities of the earthquake), the artificial energy arises

in models with coarse meshes. Regarding the running time, Abaqus/Explicit computes Δt at each increment and updates the value based on the current distortion of the elements. Thus, the analysis may last more time when the elements start changing their dimension due to the deformations, as it was the case for the highest seismic action.

10. CONCLUSION

Explicit solutions are an alternative for solving problems where the interactions between the structural elements have a strong nonlinearity relationship, as in the present case in which the behaviour of the material is brittle and the connections between walls and joists represent convergence issues for implicit solutions given the drastic change of stiffness from compression to tension.

For dynamic analysis with high nonlinearities and displacements, the mesh refinement and regularity of the elements should be considered for models with reduced integration elements. A coarse mesh reduces the computational cost, but nonreal distortions may arise and propagate easily. Despite hourglass controls can be applied to minimize the unrealistic modes, the artificial energy can be large if coarse meshes are used. The solution is to generate a more refined mesh, mainly on those parts of the model that are subjected to large deformations and stresses due to the artificial energy generated is minor. On the other hand, more elements in the model increase the computational demand since the set of equations is larger and the increment time Δt is related to the size of the smallest element. Thus, a combination of mesh size and hourglass controls should be addressed to obtain accurate or acceptable results.

Some issues that are still on discussion in the scientific community is the application of a more suitable damping technique that can control the high frequencies and the time efficient. Therefore, explicit solutions should be used carefully for the seismic analysis of buildings. Additionally, more parametric analyses and comparison between explicit and implicit solvers for unreinforced masonry buildings are required. The results could serve to develop guidelines for users during the process of modelling, analysis and postprocessing of data.

11. REFERENCES

[1] Harewood, F.J.; McHugh P.E. – Comparison of the implicit and explicit finite element methods using crystal plasticity. Computational Materials Science 2007, 39:481–94. https://doi.org/10.1016/j.commatsci.2006.08.002.

[2] Zheng G, Nie H, Chen J, Chen C, Lee HP. – “Dynamic analysis of lunar lander during soft landing using explicit finite element method” em *Acta Astronautica*, 2018, 148:69–81. https://doi.org/10.1016/j.actaastro.2018.04.014.

[3] Tarque N.; Camata G.; Spacone E.; Varum H.; Blondet M.; – “Nonlinear dynamic analysis of a full scale unreinforced adobe model” em *Earthquake Spectra* 2014, 30:1643–61. https://doi.org/10.1193/022512EQS053M.

[4] Yang B. – *Comparisons of implicit and explicit time integration methods in finite element analysis for linear elastic material and quasi-brittle material in dynamic problems*. Master thesis. Delft University of Technology, 2019.

[5] Noor-E-Khuda S.; Dhanasekar M.; Thambiratnam D.P; – "An explicit finite element modelling method for masonry walls under out-of-plane loading" em *Engineering Structures* 2016, 113:103–20. https://doi.org/10.1016/j.engstruct.2016.01.026.

[6] Dassault Systemes Simulia Corp. Abaqus/CAE 2019 2018.

[7] Boulbes R.J. – *Troubleshooting Finite-Element Modeling with Abaqus With Application in Structural Engineering Analysis.* 2010. https://doi.org/https://doi.org/10.1007/978-3-030-26740-7.

[8] Dassault Systèmes. Abaqus Analysis User's Guide 2016.

[9] Chávez M.M.; Durán D.; Peña F.; García N. – "Caracterización mecánica de muestras de mampostería extraídas de templos conventuales mexicanos del siglo XVI" em *Construction Pathology, Rehabilitation Technology and Heritage Management*, 2020.

[10] Guzmán J.A.S. – *Fichas técnicas sobre características tecnológicas y usos de maderas comercializadas en México.* 2007, 91–2.

[11] D'Altri A.M.; Cannizzaro F.; Petracca M.; Talledo D.A. – "Nonlinear modelling of the seismic response of masonry structures: Calibration strategies" em *Bulletin of Earthquake Engineering* 2022, 20:1999–2043. https://doi.org/10.1007/s10518-021-01104-1.

[12] Acito M.; Bocciarelli M.; Chesi C.; Milani G. – "Collapse of the clock tower in Finale Emilia after the May 2012 Emilia Romagna earthquake sequence: Numerical insight" em *Engineering Structures* 2014;72:70–91. https://doi.org/10.1016/j.engstruct.2014.04.026.

[13] Castellazzi G.; D'Altri A.M; de Miranda S.; Chiozzi A.; Tralli A. – "Numerical insights on the seismic behavior of a nonisolated historical masonry tower" em *Bulletin of Earthquake Engineering* 2018, 16:933–61. https://doi.org/10.1007/s10518-017-0231-6.

[14] D'Altri A.M.; Messali F.; Rots J.; Castellazzi G.; de Miranda S. – "A damaging block-based model for the analysis of the cyclic behaviour of full-scale masonry structures" em *Engineering Fracture Mechanics* 2019, 209:423–48. https://doi.org/10.1016/j.engfracmech.2018.11.046.

[15] Chopra A.K. – *Dynamics of structures. Theory and applications to earthquake engineering*. Prentice Hall, 2014.

[16] Chen X.; Duan J.; Qi H.; Li Y. – "Rayleigh damping in Abaqus/Explicit dynamic analysis" em *Applied Mechanics and Materials* 2014;627:288–94. https://doi.org/10.4028/www.scientific.net/AMM.627.288.

[17] Lemos J.V.; Dawson E.M.; Cheng Z. (*in press*) – "Application of Maxwell damping in the dynamic analysis of masonry structures with discrete elements" em *International*

Journal of Masonry Research and Innovation 2021. https://doi.org/10.1504/IJMRI.2021.10043266.

[18] Lourenço P.B.; Gaetani A. – *Finite Element Analysis for Building Assessment; Advanced Use and Practical Recommendations*. 1st ed. New York: Routledge, Taylor & Francis Group, 2022.

[19] Mostafawi H. – *Experimental and Numerical Analysis of the Shear Ring*. KTH Engineering Sciences, 2014.

[20] Martin O. – *Comparison of different Constitutive Models for Concrete in ABAQUS/Explicit for Missile Impact Analyses*. 2010. https://doi.org/10.2790/19763.

[21] Storheim M.; Notaro G.; Johansen A.; Amdahl J. – "Comparison of ABAQUS and LS-DYNA in simulations of ship collisions" em *Proceedings of the ICCGS*, Ulsan, 2016.

[22] Guerreiro J.D.C. – *Simulação dos ensaios mecânicos de provetes obtidos por fabrico aditivo*. Master. Universidade Nova de Lisboa, 2019.

[23] Moretti M.; Abruzzese L.; Augliera P.; Azzara R. – *Terremoto in Emilia Romagna: le attività del Pronto Intervento Sismico durante il primo mese di emergenza. Modalità e tempistica*. Quaderni Di Geofisica 2013.